International Journal of Biochemistry and Cell Biology 117 (2019) 105640

Contents lists available at ScienceDirect

International Journal of Biochemistry and Cell Biology

journal homepage: www.elsevier.com/locate/biocel

Endocytic degradation of ErbB2 mediates the effectiveness of neratinib in the suppression of ErbB2-positive ovarian cancer

Shanshan Wang[a,1], Jinrui Zhang[a,1], Taishu Wang[a,1], Feng Ren[a], Xiuxiu Liu[a], Yongqi Lu[a], Linying Xu[a], Yang Zhang[a], Duchuang Wang[a], Lu Xu[a], Yueguang Wu[a], Fang Liu[a], Qiong Li[a], Mohamed Y. Zaky[a,b], Shuyan Liu[a], Weijie Dong[c], Fang Liu[a,d,**], Kun Zou[e,***], Yingqiu Zhang[a,*]

[a] The Second Affiliated Hospital, Institute of Cancer Stem Cell, Dalian Medical University, Dalian, China
[b] Molecular Physiology Division, Department of Zoology, Faculty of Science, Beni-Suef University, Egypt
[c] College of Basic Medical Sciences, Dalian Medical University, Dalian, China
[d] Department of Oncology, Second Affiliated Hospital, Dalian Medical University, Dalian, China
[e] Department of Radiotherapy Oncology, the First Affiliated Hospital of Dalian Medical University, Dalian, China

ARTICLE INFO

Keywords:
ErbB2
Neratinib
Ovarian cancer
Endocytic degradation
Targeted therapy

ABSTRACT

The tyrosine kinase receptor ErbB2 is frequently found to be overexpressed in multiple cancer types. Targeted therapeutic approaches against ErbB2 have shown promising results and received FDA approvals in the treatment of breast cancer. However, this approach has not been granted in ovarian cancers till now. In order to assess the validity of ErbB2-targeted therapy in ovarian cancer, we investigated the effectiveness of two FDA-approved tyrosine kinase inhibitors of ErbB2, lapatinib and neratinib, on the growth of ovarian cancers. We observed that both lapatinib and neratinib displayed inhibitory effects towards the proliferation and migration of ErbB2-positive ovarian cancer cells *in vitro*, with neratinib showing stronger suppression in general. Neratinib treatment led to the reduction of ErbB2 protein levels, with concomitant attenuation of the phosphorylation of AKT, MEK, and ERK1/2. Immunofluorescence assays revealed that neratinib induced the internalization and lysosomal degradation of ErbB2, which was accompanied by its hyperubiquitylation. Lapatinib and neratinib also repressed the *in vivo* growth of SKOV3 cells, and neratinib downregulated ErbB2 levels in xenograft tumors to cause potent inhibition. Therefore, the ubiquitylation-mediated endocytic degradation of ErbB2 incurred by neratinib treatment conferred potent inhibition of ovarian cancer growth. Clinical investigations of neratinib in ErbB2-positive ovarian cancer are warranted.

1. Introduction

Ovarian cancer is a frequently observed type of malignancy from the department of gynecology. The mortality caused by ovarian carcinoma accounts for about 4.4% of newly diagnosed cancer-related deaths worldwide of women (Bray et al., 2018). Unfortunately, ovarian cancers are often diagnosed at the advanced stages of the disease and thus patients are generally predicted to have poor prognoses. In the clinical treatment of ovarian cancers, chemotherapies with the platinum and taxane classes of drugs have remained the major option for decades (Grunewald and Ledermann, 2016). However, recent advances in targeted therapies have significantly improved patient prognoses in the clinical management of ovarian cancers, and therefore drugs targeting the DNA damage repair pathway and the angiogenesis process in ovarian cancers have been approved by the Food and Drug Administration (FDA) (Crafton et al., 2016; Chase et al., 2017; Colombo et al., 2016). Inspired by the success of the PARP inhibitors, including olaparib, rucaparib, and niraparib, as well as the VEGF antibody bevacizumab, alternative therapeutic targets of ovarian cancers are under intensive investigations (Lin and Kraus, 2017; Staropoli et al., 2016).

* Corresponding author at: Institute of Cancer Stem Cell, Dalian Medical University, 9 West Sec. Lvshun South Road, Dalian, Liaoning Province, 116044, China.
** Corresponding author at: Department of Oncology, The Second Affiliated Hospital, Dalian Medical University, 467 Zhongshan Road, Dalian, Liaoning Province, 116011, China.
*** Corresponding author at: Department of Radiotherapy Oncology, The First Affiliated Hospital of Dalian Medical University, 222 Zhongshan Road, Dalian, Liaoning Province, 116011, China.
E-mail addresses: liufang_dy@sina.com (F. Liu), zoukun29@163.com (K. Zou), zhangyingqiu.no.1@163.com (Y. Zhang).
[1] These authors contributed equally

https://doi.org/10.1016/j.biocel.2019.105640
Received 27 August 2019; Received in revised form 25 October 2019; Accepted 28 October 2019
Available online 02 November 2019
1357-2725/

ErbB2, also known as Her2, is a receptor tyrosine kinase from the ErbB receptor family (Citri and Yarden, 2006). The overexpression of ErbB2 is recurrently observed in many types of malignancies, including breast, ovarian, and gastric cancers. The aberrant upregulation of ErbB2 confers cancer cells with various invasive properties and generally predicts the poor prognoses of patients. Nevertheless, the dominant role of ErbB2 overexpression in these cancers provides an ideal therapeutic target for clinical intervention, and different approaches of ErbB2 suppression have entered clinical applications (Rimawi et al., 2015; Segovia-Mendoza et al., 2015). Major progressions of ErbB2-targeted therapies have been achieved in the clinical treatment of ErbB2-positive breast cancer, in which antibodies and small molecule inhibitors that block ErbB2 signalling have shown significant clinical benefits and therefore have received FDA approvals. In light of the small molecule tyrosine kinase inhibitors of ErbB2, lapatinib and neratinib have been approved in the clinical treatment of breast cancers with ErbB2 overexpression.

Regarding ovarian cancer, although the aberrant overexpression of ErbB2 is also repeatedly detected from patient tissues, so far ErbB2-targeted therapy has not been approved by the FDA in the clinical treatment of ovarian cancers. In order to explore the feasibility of ErbB2-targeted therapy in ovarian cancers, we evaluated the effectiveness of two FDA-approved small molecule inhibitors against ErbB2, lapatinib and neratinib, in the suppression of ErbB2-positive ovarian cancer growth. Our observations revealed that, compared to lapatinib, the recently approved neratinib elicited a significantly stronger inhibition towards the growth of ErbB2-positive ovarian cancers both *in vivo* and *in vitro*. Additionally, the effectiveness of neratinib was associated with the endocytic degradation of ErbB2. The present study therefore provides evidence that targeting ErbB2 through neratinib will potentially show efficacy in the clinical management of ErbB2-positive ovarian cancers.

2. Materials and methods

2.1. Antibodies and reagents

Mouse anti-ErbB2 (A-2) antibody was purchased from Santa Cruz Biotechnology (CA, USA). Rabbit anti-phospho-AKT (Ser473), rabbit anti-phospho-MEK1/2 (Ser217/221), and rabbit anti-phospho-p44/42 MAPK (Erk1/2) (Thr202/Tyr204) antibodies were purchased from Cell Signaling Technology. Mouse anti-β-Actin and mouse anti-GAPDH antibodies were purchased from Proteintech (Wuhan, China). Mouse anti-α-Tubulin antibody was obtained from Sigma. Mouse anti-Ubiquitin (P4G7) antibody was obtained from Covance. Infrared-labeled secondary antibodies for immunoblottings (goat anti-mouse and anti-rabbit) were purchased from Licor. Alexa Fluor®-conjugated secondary antibodies for immunofluorescence were purchased from Invitrogen. Chloroquine was purchased from Sigma. Lapatinib (GW-572016) and neratinib (HKI-272) were purchased from Dalian Meilun Biotechnology Co. Ltd.

2.2. Cell culture

Human normal ovarian cell and ovarian cancer cells were maintained in a humidified incubator (Thermo) at 37 °C with a CO_2 concentration of 5%. The normal ovarian cell line T80 was a generous gift from Dr. Jin Q. Cheng (H. Lee Moffitt Cancer Center, USA), and was maintained in Dulbecco's modified Eagle's medium (DMEM, Gibco, USA). The growth media for ovarian cancer cell lines were as follows: HeyA8, CaOV3, and OVCAR8 cells were cultured in DMEM (Gibco, USA); SKOV3 cells were cultured in McCoy's 5A (Gibco, USA); A2780, OVCAR3, OVCAR4, OV2008, and IGROV cells were cultured in RPMI 1640 (Gibco, USA); PA-1 was cultured in Eagle's minimum essential medium (EMEM, Gibco, USA). All media were supplemented with 10% of foetal bovine serum (ExCell Bio, Shanghai) and 1% antibiotics (penicillin/streptomycin, Thermo Fisher Scientific).

2.3. Cell lysis and Western blotting

Cultured cells were washed with ice-cold PBS, before lysis with the RIPA buffer (10 mM Tris − HCl pH 7.5, 100 mM NaCl, 50 mM NaF, 0.1% (w/v) SDS, 1% (w/v) Nonidet P-40, 1% (w/v) sodium deoxycholate), which was supplemented with phosphatase and protease inhibitor cocktails as described previously (Tian et al., 2015). The cell lysates were centrifuged to clear aggregates, and protein concentrations were determined using the BCA protein assay kit (Thermo). Equal amounts of proteins were separated on SDS-PAGE gels and samples were electro-transferred to nitrocellulose membranes (Merck Millipore). The membranes were blocked with 4% non-fat milk in PBS for 1 h at room temperature, before incubation with primary antibodies for overnight at 4 °C. The following day, blots were washed three times with PBS and then incubated with secondary antibodies with infrared labeling at 680 nm or 800 nm. After PBS washes, membranes were finally scanned using a LICOR Odyssey Imager. Acquired data were analyzed using Image Studio software (LICOR) according to manufacturer's instructions.

2.4. Immunofluorescence

Ovarian cancer cells were cultured on glass coverslips in 35 mm dishes. Cells were treated with lapatinib (200 nM), neratinib (200 nM), or DMSO as control. For immunofluorescence assays, cells were washed with PBS for three times and fixed with 4% (w/v) paraformaldehyde (Sigma). Then cells were permeabilized with 0.2% Triton X100 and blocked by 2% goat serum for 30 min at room temperature, followed by incubation with primary antibodies for 30 min. After PBS washes, cells were stained with fluorescent secondary antibodies at room temperature for 30 min. The coverslips were mounted onto slide using Mowiol supplemented with DAPI to stain the nucleus. Cells were finally observed under a fluorescent microscope (Olympus BX63, Japan).

2.5. Immunoprecipitation assay

Immunoprecipitation assay was performed as described previously (Zhang et al., 2016). In brief, SKOV3 cells were treated with lapatinib, neratinib, or DMSO as control for 24 h. Cell lysates were prepared using the RIPA buffer as mentioned above. Protein concentration was measured with the BCA assay (Pierce). Equal amounts of cell lysates from each condition (0.5 mg) were incubated with protein G-agarose (Roche) and anti-ErbB2 (A-2, Santa Cruz) antibody at 4 °C for 4 h. Immunoprecipitates were then washed with the YP-IP buffer (150 mM NaCl, 10 mM Tris − HCl pH 7.5, 0.1% Nonidet P-40) for three times, followed by elution with 1.5 X SDS-PAGE loading buffer. Protein samples were finally fractionated on 6% SDS-PAGE gels, and subsequently subjected to immunoblotting analysis with anti-ErbB2 and anti-Ubiquitin antibodies.

2.6. MTT assay

Ovarian cancer SKOV3 and IGROV cells were seeded into 96-well plates at a density of 2500 cells per well. The next day, cells were treated with DMSO, lapatinib (200 nM), or neratinib (200 nM) for 72 h. As previously described, 20 μl of 3-(4, 5-Dimethylthiazol-2-yl)-2, 5-diphenyltetrazolium bromide (MTT) were added into each well to reach a final concentration of 0.5 mg/ml, and plates were returned for incubation at 37 °C for 3 h (Wang et al., 2017). Then media were removed and 150 μl of dimethylsulfoxide (DMSO) were added into each well to dissolve formazan. The absorbance was finally recorded using a spectrometer (PerkinElmer) at both 570 and 630 nm.

2.7. Colony formation assay

SKOV3 and IGROV cells were plated onto 35 mm dishes (800 cells per dish) and maintained in the incubator for 4 days, before treated with lapatinib and neratinib (both at 200 nM) for one week with the drugs replenished every 24 h. After the removal of culture media, SKOV3 and IGROV cells were washed with PBS for three times prior to methanol fixation. The cells were then immediately stained using 1% crystal violet for 15 min. Finally, images were collected using a Bio-Rad imaging System and analyzed using Image *J* software to calculate the number and size of colonies formed from each condition.

2.8. Wound healing assay

Wound healing assay was conducted as described previously (Khan et al., 2015). Briefly, SKOV3 and IGROV cells were seeded onto 35 mm dishes to grow into a confluent monolayer, which was then gently scratched by a 200 µl pipette tip. The dishes were then washed with PBS to remove all detached cells. Fresh media supplemented with lapatinib (200 nM), neratinib (200 nM), or DMSO were added in the presence of mitomycin at 5 µg/ml to inhibit cell proliferation. All plates were placed back into the incubator and images were taken at indicated times using a phase contrast microscope (Leica, Germany). To quantify the distances cells travelled during incubation, three random regions across the wounds were used in the measurement.

2.9. Cell cycle analysis

SKOV3 and IGROV cells were treated with lapatinib (200 nM), neratinib (200 nM), or DMSO as control for 24 h before collection. One million cells from each condition were counted and fixed with 70% ice-cold ethanol for overnight. Subsequently, cells were stained with 20 µg/ml of propidium iodide in the presence of 100 µg/ml of RNase A and 0.1% of Triton X100 for 15 min at 37 °C in the dark. The samples were finally analyzed using a bench top flow cytometer (ACCURI C6, BD Bioscience) and acquired data were analyzed using FlowJo software (version 7.6.1).

2.10. Sphere formation

SKOV3 and IGROV cells were plated into ultra-low attachment 96-well plates, and maintained in DMEM/F12 medium contain 20 ng/ml of human basic fibroblast growth factor, 20 ng/ml of epidermal growth factor, and 2% B27. Cells were maintained in the incubator for 3 consecutive days, and then treated with lapatinib and neratinib (both at 200 nM) for 6 days. The spheres were imaged using a phase contrast microscope (Leica, Germany) and images were analyzed using ImageJ software to calculate the sizes from each condition.

2.11. Xenograft mouse model

Animal experiments were performed in accordance with the 1996 National Institutes of Health Guide for the Care and use of Laboratory Animals, and the procedures were approved by the Institutional Animal Care and Use Committee of the Dalian Medical University. To generate xenograft mouse models, SKOV3 cells (1 million/mouse) were inoculated subcutaneously into athymic female nude mice (4–6 weeks old Balb/c background, Vital River Laboratories, Beijing). Mice were then maintained in the laminar airflow cabinets under specific pathogen-free conditions, provided with access to irradiated pellet food and sterilized water. The sizes of the xenograft tumors were measured using a vernier caliper every 2 days. One week later, the mice carrying xenografts of similar sizes were randomly divided into 3 groups (5 mice per group), which were treated with lapatinib, neratinib, and vehicle as control. Lapatinib was dissolved in 2% DMSO, 30% PEG 300, and 5% Tween 80 in distilled water, while neratinib was solubilized in 30% PEG 400, 0.5% Tween 80, and 5% Propylene glycol in distilled water. Lapatinib and neratinib were administered through daily oral gavage for 14 consecutive days at dosages of 100 mg/kg and 40 mg/kg, respectively. Tumor xenografts were excised from the mice after sacrifice, and processed for Western blotting analyses.

2.12. Statistical analysis

All experiments were carried out at least 3 times with biological repeats. To assess statistical differences between samples, Student's *t*-test was performed using GraphPad Prism software (version 5.01) to generate *p* values. A *p* value less than 0.05 was considered as statistically significant difference. Quantitation data were presented as mean ± standard error of the mean (SEM).

3. Results

3.1. Lapatinib and neratinib suppress signal transduction emanating from ErbB2

In order to identify ErbB2-positive ovarian cancer cells, we conducted Western blotting analyses using a panel of 10 ovarian cancer cell lines, together with the normal ovarian T80 cells as control. As illustrated in Fig. 1A, the normal ovarian T80 cells expressed very low levels of ErbB2. Similarly, comparable expressions of ErbB2 were detected from ovarian cancer CaOV3, OVCAR3, OVCAR4, and PA-1 cells, while A2780, OVCAR8, OV2008, and HeyA8 cells expressed slightly more ErbB2 proteins (Fig. 1A). On the contrary, ovarian cancer SKOV3 and IGROV cells contained considerably elevated levels of ErbB2, especially in SKOV3 cells from which abundant ErbB2 was observed (Fig. 1A). We therefore selected SKOV3 and IGROV cells to investigate the effects of ErbB2 inhibition by lapatinib and neratinib.

To examine the influence of both inhibitors on the signals transmitted from ErbB2, we first titrated a range of concentrations for both lapatinib and neratinib in SKOV3 and IGROV cells, Western blotting was performed to detect the effect of both inhibitors on ErbB2 expression (Fig. S1), and immunofluorescence was used to examine ErbB2 subcellular localization upon lapatinib and neratinib treatment in presence of chloroquine (Fig. S2), from which we observed that a concentration of 200 nM for both inhibitors showed adequate inhibition on ErbB2 and downstream signaling. It has also been established that both lapatinib and neratinib inhibit cancer cell proliferation at nM ranges. To avoid the off target effects incurred by usage of both inhibitors at too high concentrations, also considering that the blood concentration of neratinib is about 150 nM, we selected 200 nM for both inhibitors to perform in vitro. Then we treated SKOV3 and IGROV cells with lapatinib and neratinib (both at 200 nM after titration validation) for 12 and 24 h, and then performed Western blotting analyses to detect the activation of AKT, MEK, and ERK1/2 that were key signalling modules downstream of ErbB2. The results showed that, in SKOV3 cells, both inhibitors strongly suppressed the activation of ERK1/2, and neratinib but not lapatinib caused the significant inhibition of the phosphorylation of AKT and MEK (Fig. 1B, E, and F); while in IGROV cells, the two inhibitors elicited similar suppression of the activation of AKT, MEK, and ERK1/2 (Fig. 1C, H, and I). It is intriguing that lapatinib and neratinib, in both SKOV3 and IGROV cells, displayed opposite effects on the expression levels of ErbB2: lapatinib treatment elevated the expression of ErbB2, while neratinib strongly decreased the protein levels of ErbB2 (Fig.1B-D and G).

In addition, lapatinib is a selective inhibitor targeting EGFR, ErbB2, and ErbB4 with IC50 values of about 10 nM for EGFR and ErbB2, while an IC50 of over 350 nM for ErbB4 in cell free assays (Rusnak et al., 2001). On the other hand, neratinib is a specific inhibitor for only EGFR and ErbB2 with IC50 values of 50–100 nM (Rabindran et al., 2004). As abovementioned, we have tested the inhibitory effects of both inhibitors using a series of working concentrations and decided to use 200 nM for both inhibitors. At 200 nM concentration for lapatinib and

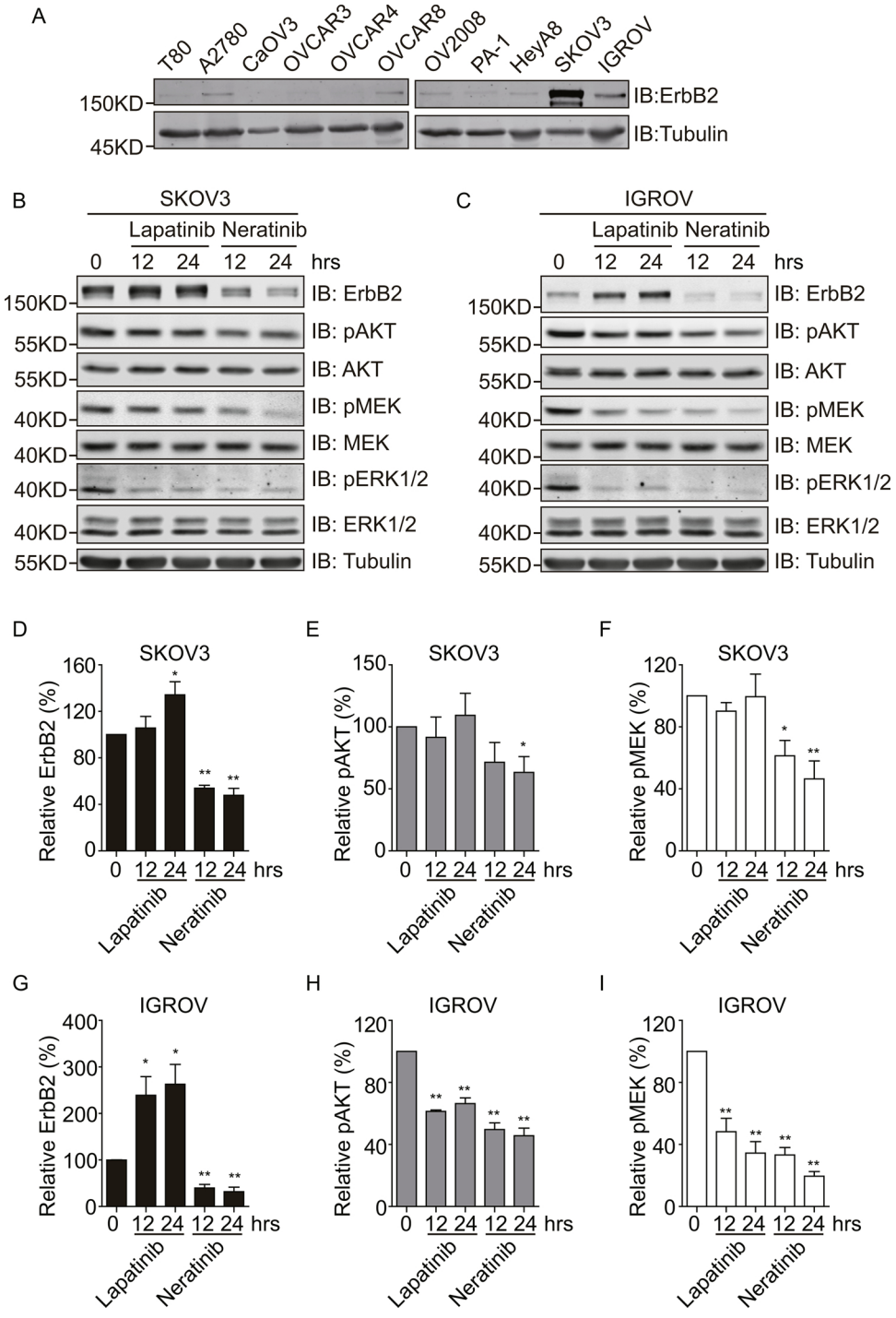

Fig. 1. The effects of lapatinib and neratinib on ErbB2 levels and its downstream signalling. (A) Cultured ovarian cell lines as indicated were lysed to prepare protein samples, from which ErbB2 expression levels were examined by immunoblotting analyses. Tubulin was used as loading control. Cultured SKOV3 (B) and IGROV (C) cells were treated with lapatinib and neratinib (both at 200 nM) for 12 and 24 h, before lysed as described in the methods. Cell lysates were analyzed by immunoblotting with indicated antibodies. Tubulin was probed to show equal loading. The expression levels of ErbB2, pAKT, and pMEK in SKOV3 cells were quantified from 3 independent experiments, and the averages of relative values to corresponding untreated control samples were shown in (D), (E), and (F), respectively. Similarly, the quantification data of ErbB2, pAKT, and pMEK from IGROV cells were illustrated in (G), (H), and (I), respectively. All error bars represent the standard error of the mean (n = 3), with * and ** indicating $p < 0.05$ and $p < 0.01$, respectively.

neratinib, the main targets for both inhibitors are EGFR and ErbB2. Therefore, in addition to ErbB2, we also examined the effects of lapatinib and neratinib on EGFR. As shown in Fig. S1A and B, at 200 nM both inhibitors showed no influence on EGFR expression.

3.2. ErbB2 kinase inhibition deters the proliferation of ErbB2-positive ovarian cancer cells

We next evaluated the impact of lapatinib and neratinib on the growth of ErbB2-positive ovarian cancer cells by conducting MTT and colony formation assays. Results from MTT assays showed that, compared to lapatinib-treated cells, neratinib-treated group showed significantly reduced growth than control group in SKOV3 cells; while both lapatinib and neratinib treatment led to the significant inhibition of the propagation of IGROV cells, with a stronger effect observed by neratinib (Fig. 2A). In accordance with data from MTT assays, the results from colony formation assays revealed a stronger inhibitory effect of neratinib on both SKOV3 and IGROV cells compared to lapatinib treatment (Fig. 2B and C). In the subsequent flow cytometry analyses, we investigated the impact of lapatinib and neratinib on the cell cycle distribution of ErbB2-positive SKOV3 and IGROV cells. As described in Fig. 2D-F, lapatinib treatment resulted in a significant reduction of IGROV cells distributed in the S phase of the cell cycle, but failed to cause significant change in SKOV3 cells; while neratinib treatment significantly increased both SKOV3 and IGROV cells distributed at the G1 phases, with corresponding decreases at the S phases.

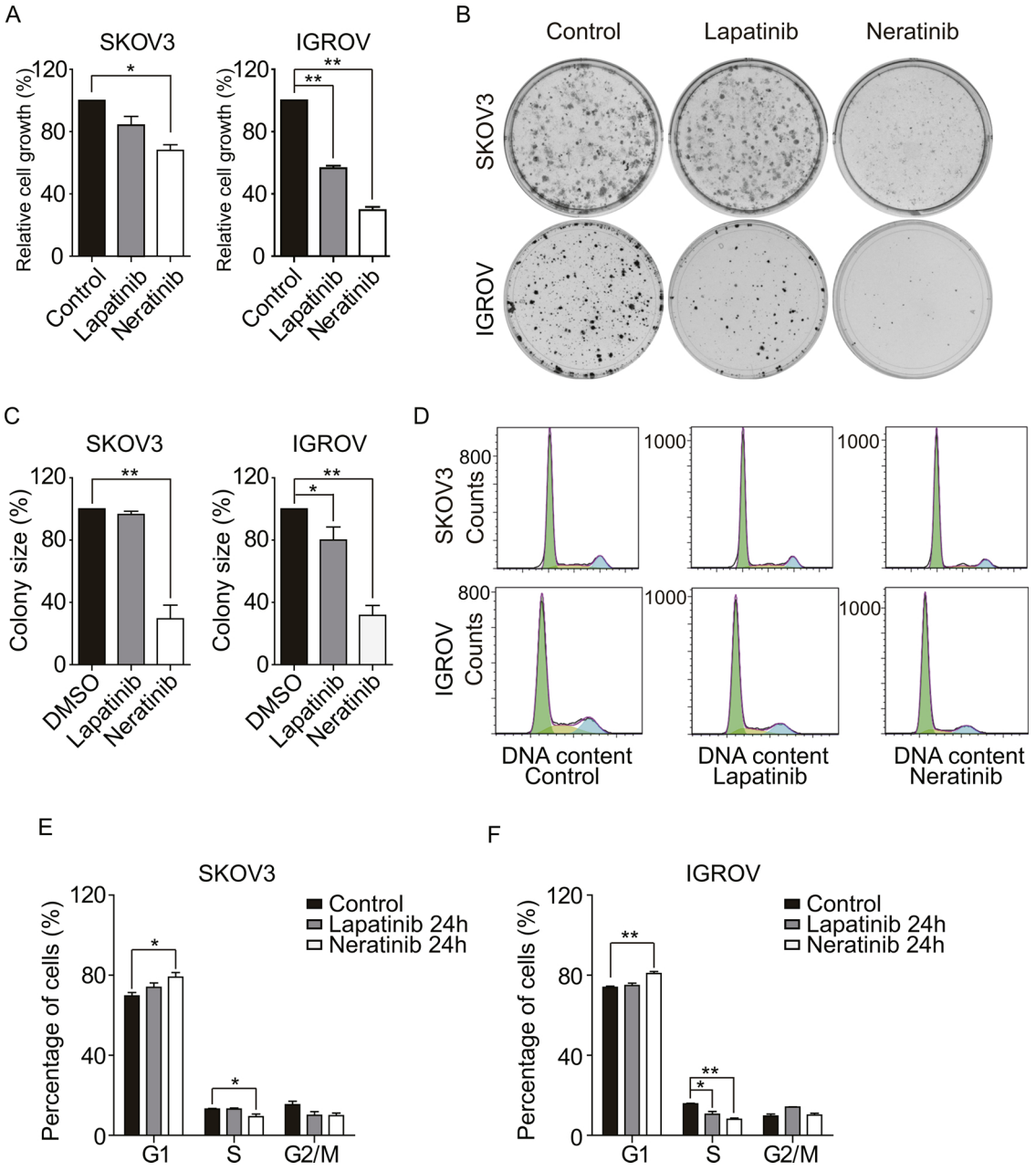

Fig. 2. Kinase inhibitors suppress the cell propagation and cell cycle progression of SKOV3 and IGROV cells. (A) Cultured SKOV3 and IGROV cells were treated with 200 nM of lapatinib or neratinib, and DMSO as control for 72 h. Cell proliferation was then measured by carrying out MTT assays. Quantification data show the relative cell growth rates from 3 independent experiments. (B) Representative images of colony formation assays performed as described in the method section, and (C) shows the quantification data of colony sizes in SKOV3 and IGROV groups by measuring colonies from 3 randomly chosen views. (D) Representative histograms of cell cycle distribution of lapatinib and neratinib-treated SKOV3 and IGROV cells, with control groups treated with DMSO. (E) and (F) show the quantification of the percentages of cells distributed at G1, S, and G2/M stages during the cell cycle in SKOV3 and IGROV cells, respectively. All error bars represent the standard error of the mean (n = 3), with * and ** indicating $p < 0.05$ and $p < 0.01$, respectively.

3.3. Lapatinib and neratinib inhibit cell migration and sphere formation

To examine the influence of lapatinib and neratinib on the cell migration of ErbB2-positive ovarian cancers, we conducted wound healing assays using SKOV3 and IGROV cells. Since both tyrosine kinase inhibitors deterred cell propagation, we added mitomycin (5 μg/ml) to block cell cycle progression in this assay to remove the contribution of their effects on cell proliferation. As illustrated in Fig. 3A-D, results from the wound healing assays revealed that, in SKOV3 cells, control and lapatinib-treated cells recovered more than 60% of the wound after 36 h, but neratinib-treated group accomplished only less than 50%; and in IGROV cells, control cells closed nearly 60% of the gap after 60 h of incubation, while lapatinib and neratinib-treated groups only managed to recover 33% and 15% on average, respectively. These data indicated that, compared to lapatinib, neratinib is more potent in the suppression of ovarian cancer cell migration.

Given that anchorage-independent growth is an important feature of cancer cells, we tested the impact of lapatinib and neratinib on this process by carrying out sphere formation assays with SKOV3 and IGROV cells. As shown in Fig. 3E, both inhibitors strongly repressed the formation of tumor spheres in both SKOV3 and IGROV cells. After 6 days of treatment, lapatinib led to 57% and 54% reductions in the average sizes of spheres formed by SKOV3 and IGROV, respectively; and neratinib resulted in an average of 82% and 75% decreases of

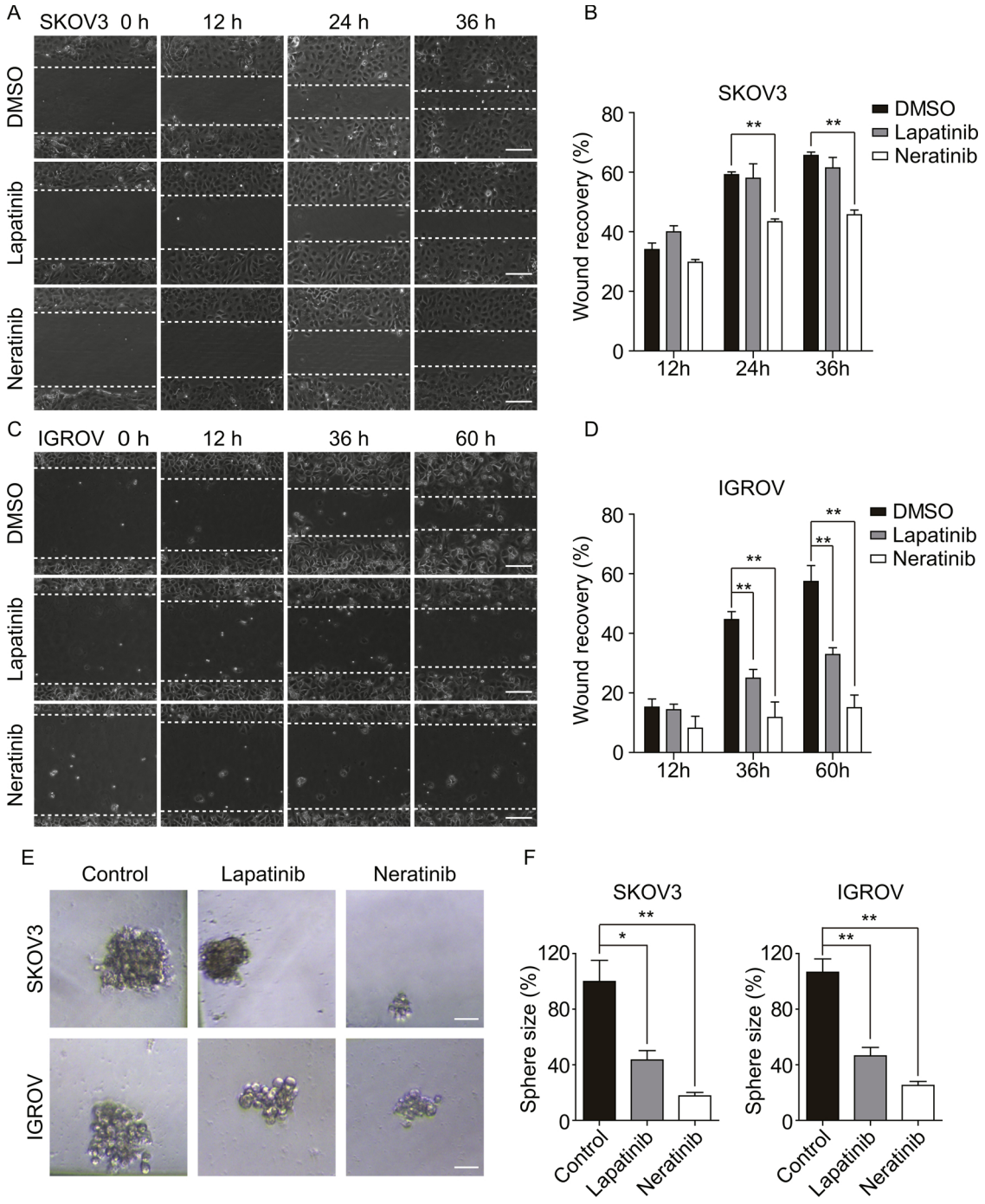

Fig. 3. The impact of lapatinib and neratinib on the cell migration and sphere formation of ErbB2-positive ovarian cancer cells. (A) SKOV3 cells were grown to form a confluent monolayer before a wound was generated. After PBS washes, cells were kept in mitomycin-containing media supplemented with lapatinib (200 nM), neratinib (200 nM), or DMSO as control. Representative images of the wound area were captured at indicated times and shown. Scale bar = 200 μm. The average distance cells migrated into the wound was quantified at indicated times and shown in (B). (C) IGROV cells were treated the same way as SKOV3 and representative images of the wound area were shown at indicated times. Scale bar = 200 μm. (D) Quantification data were acquired as in B and shown. (E) Representative images of spheres formed by SKOV3 and IGROV cells treated with lapatinib (200 nM), neratinib (200 nM), or DMSO as control. Scale bar = 40 μm. (F) shows the quantification data of relative sphere sizes from different experimental groups from E. All error bars represent the standard error of the mean (n = 3), with * and ** indicating $p < 0.05$ and $p < 0.01$, respectively.

sphere sizes in SKOV3 and IGROV cells (Fig. 3F), respectively.

3.4. Neratinib induces the endocytic degradation of ErbB2 in ovarian cancer cells

As described above, phenotypic observations revealed that, compared to lapatinib, neratinib elicited stronger inhibitory effects in ErbB2-positive ovarian cancer cells, with concomitant downregulation of ErbB2 protein levels (Fig. 1–3). A closer examination of pivotal signalling molecules downstream of ErbB2 by Western blotting showed that neratinib-induced decrease of ErbB2 expression resulted in more robust inhibition of AKT and MEK in SKOV3 cells (Fig. 1). Our previous investigation on lapatinib and neratinib in breast cancer has shown that neratinib triggered the endocytic downregulation of ErbB2 through

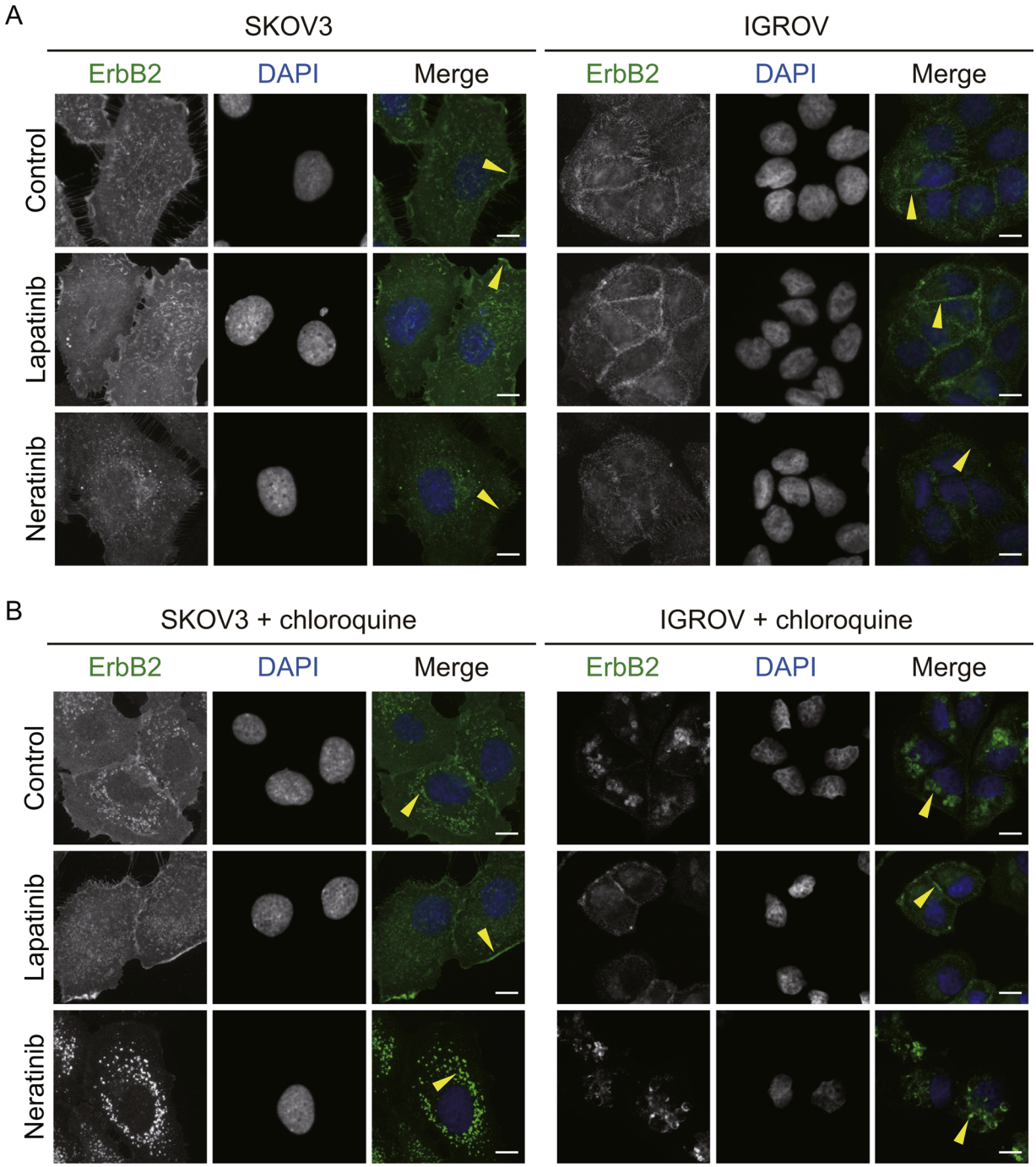

Fig. 4. Neratinib induces the internalization and lysosomal degradation of ErbB2. (A) SKOV3 and IGROV cells cultured on coverslips were treated with lapatinib (200 nM), neratinib (200 nM), or DMSO as control for 24 h. Cells were washed with PBS and processed for immunofluorescence analysis with anti-ErbB2 antibody. The nucleus was stained with DAPI. Representative fluorescent images show the distribution of ErbB2 in SKOV3 and IGROV cells, with triangles pointing to the peripheries of ovarian cancer cells. (B) Cultured SKOV3 and IGROV cells were treated with lapatinib (200 nM), neratinib (200 nM), or DMSO as control in the presence of chloroquine (100 μM) for 24 h. Cellular ErbB2 localizations were examined by immunofluorescence analysis. DAPI stains nucleus. Representative images show ErbB2 staining in chloroquine-treated SKOV3 and IGROV cells, with triangles pointing to ErbB2 signals. Scale bar = 10 μm.

promoting its ubiquitylation (Zhang et al., 2016). We therefore wondered whether this kinase inhibitor could exert similar functions in ovarian cancer cells, and thus carried out immunofluorescence experiments to examine the subcellular localization of ErbB2 receptors under lapatinib and neratinib-treated conditions. As illustrated in Fig. 4A, membrane distribution of ErbB2 is easily identifiable in both SKOV3 and IGROV cells under control and lapatinib-treated conditions, but appears to be nearly invisible in the neratinib-treated groups. Furthermore, when we blocked lysosomal degradation using chloroquine, intracellular accumulation of ErbB2 was readily discernable from the control but not lapatinib-treated groups of both SKOV3 and IGROV cells (Fig. 4B). However, in the chloroquine-treated SKOV3 and IGROV cells, neratinib caused significantly increased perinuclear staining of ErbB2, which indicated enhanced internalization and lysosomal sorting of ErbB2 (Fig. 4B). Therefore, these immunofluorescence results demonstrated that neratinib efficiently induced the endocytic degradation of ErbB2 in ovarian cancer cells.

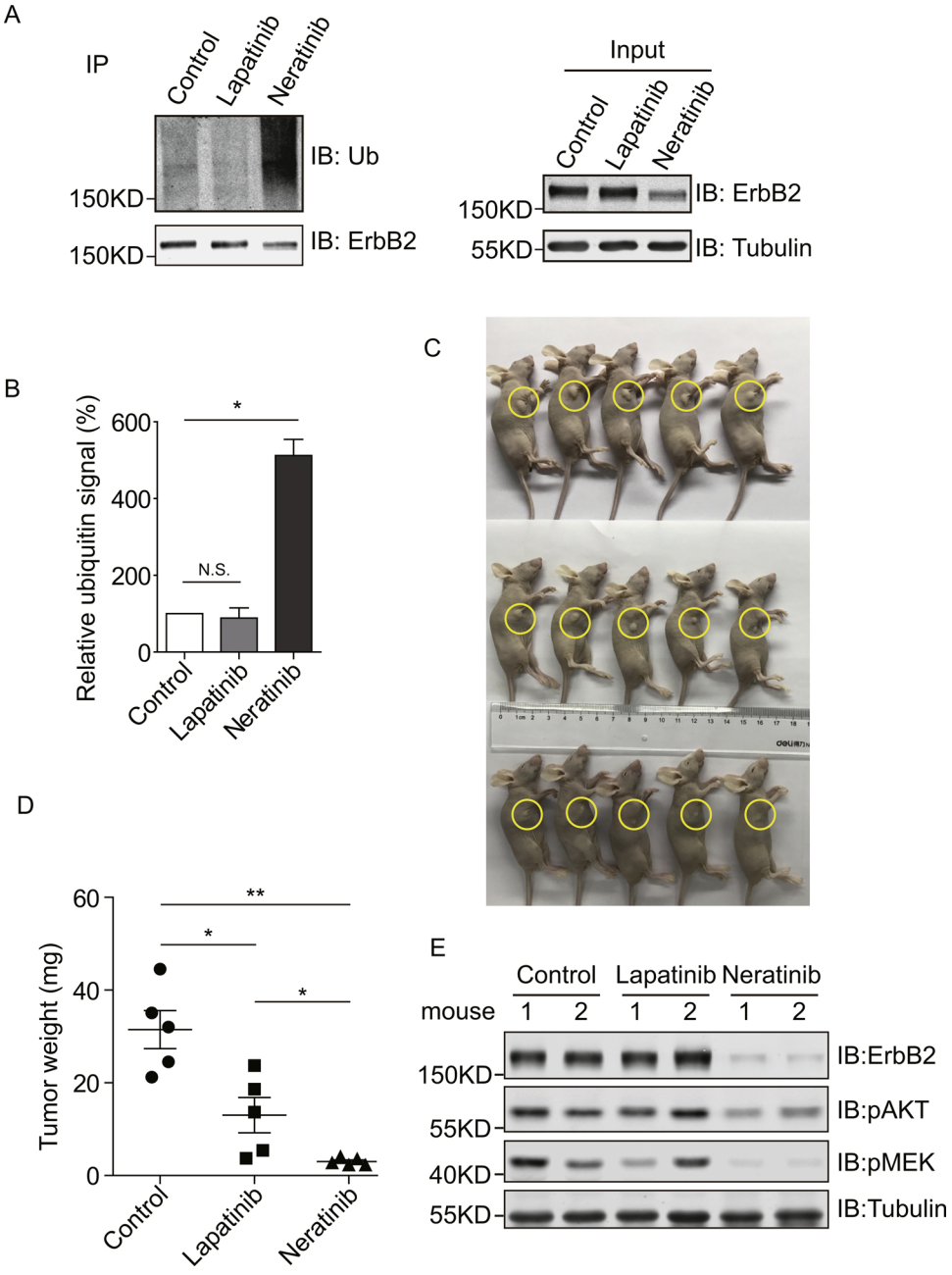

Fig. 5. Neratinib triggers ErbB2 ubiquitylation and inhibits SKOV3 xenograft tumor growth *in vivo*. (A) SKOV3 cells were treated with lapatinib (200 nM), neratinib (200 nM), or DMSO as control for 24 h before lysis. ErbB2 was immunoprecipitated from the cell lysates and analyzed by immunoblotting together with cell lysates using indicated antibodies. Tubulin was probed to show equal loading. (B) Quantification of ubiquitin signal on immunoprecipitated ErbB2 proteins from cells treated with lapatinib, neratinib, or DMSO as control. (C) Nude mice were inoculated with SKOV3 cells to form xenograft tumors, which were then treated with lapatinib or neratinib as described in the methods. Image shows xenograft tumors on nude mice (circled) from different treatment groups. (D) Quantification data of the weight of xenograft tumors. Error bars represent the standard error of the mean (n = 5), with * and ** indicating $p < 0.05$ and $p < 0.01$, respectively. (E) Protein samples were prepared from xenograft tumor tissues (2 per treatment group) and analyzed by immunoblotting using indicated antibodies. Tubulin was probed to show equal loading.

3.5. Neratinib induces ErbB2 ubiquitylation and suppresses the in vivo growth of ovarian cancer

We have previously reported a unique function of neratinib to cause the potent ubiquitylation of ErbB2 in breast cancer cells (Zhang et al., 2016). As expected, when we examined the ubiquitylation status of ErbB2 in neratinib-treated ovarian cancer cells, a remarkably enhanced ubiquitin signal on immunoprecipitated ErbB2 was detected compared to those from control and lapatinib-treated groups (Fig. 5A and B).

In order to evaluate the effectiveness of lapatinib and neratinib on the ovarian cancer growth *in vivo*, we generated xenograft mouse models using SKOV3 cells. Tumor-bearing mice were randomly divided into 3 groups and treated with lapatinib, neratinib, and vehicle as control. As shown in Fig. 5C and D, both lapatinib and neratinib treatment led to significant suppression of the growth of SKOV3 xenograft tumors, with neratinib showing stronger effects than lapatinib. We then examined the expression levels of ErbB2 and the phosphorylation status of AKT and MEK by Western blotting in xenograft tumor samples from the three groups. In accordance with data from *in vitro* studies using ovarian cancer cell lines, the protein levels of ErbB2 and activation of AKT and MEK were strongly repressed in neratinib-treated samples compared to control and lapatinib-treated ones (Fig. 5E).

4. Discussion

For decades, ovarian cancer has remained a deadly type of disease that threatens the lives of tens of thousands women every year globally (Mortality and Causes of Death, 2015). Although targeted therapies have brought new hope and have significantly prolonged the survival of ovarian cancer patients, FDA-approved druggable targets remain very limited so far in the clinical application. In the present study, we focused on ErbB2, a receptor tyrosine kinase from the EGFR family, which has already been proven to be a successful therapeutic target in cancer treatment, with multiple FDA approvals received in the clinical management of breast and gastric cancers. Considering the evidence that ErbB2 overexpression is also frequently observed in ovarian cancers, we

investigated the effectiveness of two FDA-approved small molecule inhibitors against ErbB2, lapatinib and neratinib, on the *in vivo* and *in vitro* growth of ErbB2-positive ovarian cancer.

From a panel of ovarian cancer cell lines and compared to the normal ovarian T80 cells, we observed that SKOV3 and IGROV cell lines contained high expression levels of ErbB2 (Fig. 1A). By searching the cancer cell line encyclopedia (CCLE) website for ErbB2 expression in collected ovarian cancer cell lines, we found that SKOV3 ranks the first among all others while IGROV appears as the 8th of high expression (Fig. S3). In addition, it has also been reported IGROV cells express moderate levels of ErbB2 (Wilken et al., 2010; Sain et al., 2006). Using these two ErbB2-positive ovarian cancer cell lines, we conducted a series of phenotypic assays, including cell proliferation, colony formation, cell cycle, cell migration, and sphere formation, with results showing the inhibitory effects of both lapatinib and neratinib (Fig. 2 and 3). In general, the suppression incurred by both inhibitors appeared to be stronger in IGROV than SKOV3 cells, except for sphere formation assays from which lapatinib and neratinib elicited similar inhibition. One possible explanation to these observations might be due to the expression levels of ErbB2 in SKOV3 and IGROV cells, with the former contain considerably greater amounts than the latter. Furthermore, in both SKOV3 and IGROV cells, neratinib exhibited greater potency than lapatinib, which correlated with its special competence to down regulate ErbB2 levels. Such effect of neratinib on ErbB2 distribution was confirmed by immunofluorescence data, which revealed the internalization and lysosomal accumulation of ErbB2 under neratinib-treated condition. From the mechanistic aspect, we observed that ErbB2 became highly ubiquitylated following neratinib treatment, compared to control and lapatinib-treated conditions. Consistent with data from *in vitro* studies, the *in vivo* growth of SKOV3 xenograft tumors was also significantly repressed by lapatinib and neratinib, with neratinib showing more robust inhibition; and results from the Western blotting analysis of xenograft tumors also confirmed the concurrent down-regulation of ErbB2 in neratinib-treated samples. Therefore, our findings collectively indicate that ErbB2 targeting by tyrosine kinase inhibitors, including lapatinib and neratinib, is effective in ErbB2-positive ovarian cancer; and the recently approved neratinib induces ubiquitylation-mediated endocytic degradation of ErbB2, thus leading to the potent inhibition of ovarian cancer growth.

In accordance with our observations, Puvanenthiran et al. compared different types of tyrosine kinase inhibitors against the ErbB family, and reported that neratinib was effective in the growth inhibition of ovarian cancer cells as well as in the suppression of SKOV3 cell migration (Puvanenthiran et al., 2016). Previous studies by Santin and colleagues also showed the efficacy of neratinib in the treatment of ErbB2-positive carcinosarcoma and epithelial ovarian carcinoma (Schwab et al., 2015; Menderes et al., 2017). Through comparing the effectiveness of lapatinib and neratinib on the growth of ErbB2-positive ovarian cancer *in vitro* and *in vivo*, our observations provide important mechanistic insights into the competence of neratinib, revealing its advantage of inducing ubiquitylation-mediated ErbB2 degradation in ovarian cancer. This special function of neratinib is likely attributed to its feature as an irreversible kinase inhibitor to ErbB2, in contrast to the reversible inhibitor lapatinib, allowing the covalent attachment of neratinib to the cysteine 805 residue of ErbB2 that leads to chaperone HSP90 dissociation, subsequent receptor ubiquitylation, and the resultant endocytic degradation of ErbB2 (Zhang et al., 2016; Rabindran et al., 2004; Wissner et al., 2003; Wissner and Mansour, 2008).

To summarize, our findings indicate the potential efficacy of neratinib in the treatment of ovarian cancer patients with ErbB2 overexpression. Furthermore, Dent and coworkers have reported the additional effects of neratinib in ovarian cancers, including reducing the expression of mutant N-RAS and synergizing with the PARP inhibitor niraparib (Booth et al., 2018a, b). Therefore, clinical investigations of neratinib in ErbB2-positive ovarian cancer are warranted with patient groups classified by various molecular markers to reveal its potential indications.

CRediT authorship contribution statement

Shanshan Wang: Investigation. **Jinrui Zhang:** Investigation. **Taishu Wang:** Investigation. **Feng Ren:** Investigation. **Xiuxiu Liu:** Investigation. **Yongqi Lu:** Investigation. **Linying Xu:** Investigation. **Yang Zhang:** Investigation. **Duchuang Wang:** Investigation. **Lu Xu:** Investigation. **Yueguang Wu:** Investigation. **Fang Liu:** Investigation. **Qiong Li:** Investigation. **Mohamed Y. Zaky:** Investigation. **Shuyan Liu:** Investigation. **Weijie Dong:** Investigation. **Fang Liu:** Conceptualization, Funding acquisition, Investigation. **Kun Zou:** Conceptualization, Funding acquisition, Investigation. **Yingqiu Zhang:** Conceptualization, Funding acquisition, Investigation, Writing - original draft.

Declaration of Competing Interest

The authors declare no conflict of interest.

Acknowledgment

This work was supported by the National Natural Science Foundation of China (No. 81702628 to YZ and No. 81703904 to KZ).

Appendix A. Supplementary data

Supplementary material related to this article can be found, in the online version, at doi:https://doi.org/10.1016/j.biocel.2019.105640.

References

Booth, L., Roberts, J.L., Poklepovic, A., Kirkwood, J., Sander, C., Avogadri-Connors, F., Cutler Jr., R.E., Lalani, A.S., Dent, P., 2018a. The levels of mutant K-RAS and mutant N-RAS are rapidly reduced in a Beclin1 / ATG5 -dependent fashion by the irreversible ERBB1/2/4 inhibitor neratinib. Cancer Biol. Ther. 19, 132–137.

Booth, L., Roberts, J.L., Samuel, P., Avogadri-Connors, F., Cutler, R.E., Lalani, A.S., Poklepovic, A., Dent, P., 2018b. The irreversible ERBB1/2/4 inhibitor neratinib interacts with the PARP1 inhibitor niraparib to kill ovarian cancer cells. Cancer Biol. Ther. 19, 525–533.

Bray, F., Ferlay, J., Soerjomataram, I., Siegel, R.L., Torre, L.A., Jemal, A., 2018. Global cancer statistics 2018: GLOBOCAN estimates of incidence and mortality worldwide for 36 cancers in 185 countries. CA Cancer J. Clin. 68, 394–424.

Chase, D.M., Chaplin, D.J., Monk, B.J., 2017. The development and use of vascular targeted therapy in ovarian cancer. Gynecol. Oncol.

Citri, A., Yarden, Y., 2006. EGF-ERBB signalling: towards the systems level. Nat. Rev. Mol. Cell Biol. 7, 505–516.

Colombo, N., Conte, P.F., Pignata, S., Raspagliesi, F., Scambia, G., 2016. Bevacizumab in ovarian cancer: focus on clinical data and future perspectives. Crit. Rev. Oncol. Hematol. 97, 335–348.

Crafton, S.M., Bixel, K., Hays, J.L., 2016. PARP inhibition and gynecologic malignancies: a review of current literature and on-going trials. Gynecol. Oncol.

Grunewald, T., Ledermann, J.A., 2016. Targeted therapies for ovarian Cancer. Best Pract. Res. Clin. Obstet. Gynaecol.

Khan, M.N., Wang, B., Wei, J., Zhang, Y., Li, Q., Luan, X., Cheng, J.W., Gordon, J.R., Li, F., Liu, H., 2015. CXCR1/2 antagonism with CXCL8/Interleukin-8 analogue CXCL8(3-72)K11R/G31P restricts lung cancer growth by inhibiting tumor cell proliferation and suppressing angiogenesis. Oncotarget 6, 21315–21327.

Lin, K.Y., Kraus, W.L., 2017. PARP inhibitors for Cancer therapy. Cell 169, 183.

Menderes, G., Bonazzoli, E., Bellone, S., Black, J.D., Lopez, S., Pettinella, F., Masserdotti, A., Zammataro, L., Litkouhi, B., Ratner, E., Silasi, D.A., Azodi, M., Schwartz, P.E., Santin, A.D., 2017. Efficacy of neratinib in the treatment of HER2/neu-amplified epithelial ovarian carcinoma in vitro and in vivo. Med. Oncol. 34 91.

Mortality, G.B.D., Causes of Death, C., 2015. Global, regional, and national age-sex specific all-cause and cause-specific mortality for 240 causes of death, 1990-2013: a systematic analysis for the Global Burden of Disease Study 2013. Lancet 385, 117–171.

Puvanenthiran, S., Essapen, S., Seddon, A.M., Modjtahedi, H., 2016. Impact of the putative cancer stem cell markers and growth factor receptor expression on the sensitivity of ovarian cancer cells to treatment with various forms of small molecule tyrosine kinase inhibitors and cytotoxic drugs. Int. J. Oncol. 49, 1825–1838.

Rabindran, S.K., Discafani, C.M., Rosfjord, E.C., Baxter, M., Floyd, M.B., Golas, J., Hallett, W.A., Johnson, B.D., Nilakantan, R., Overbeek, E., Reich, M.F., Shen, R., Shi, X., Tsou, H.R., Wang, Y.F., Wissner, A., 2004. Antitumor activity of HKI-272, an orally active, irreversible inhibitor of the HER-2 tyrosine kinase. Cancer Res. 64, 3958–3965.

Rimawi, M.F., Schiff, R., Osborne, C.K., 2015. Targeting HER2 for the treatment of breast

cancer. Annu. Rev. Med. 66, 111–128.
Rusnak, D.W., Lackey, K., Affleck, K., Wood, E.R., Alligood, K.J., Rhodes, N., Keith, B.R., Murray, D.M., Knight, W.B., Mullin, R.J., Gilmer, T.M., 2001. The effects of the novel, reversible epidermal growth factor receptor/ErbB-2 tyrosine kinase inhibitor, GW2016, on the growth of human normal and tumor-derived cell lines in vitro and in vivo. Mol. Cancer Ther. 1, 85–94.
Sain, N., Krishnan, B., Ormerod, M.G., De Rienzo, A., Liu, W.M., Kaye, S.B., Workman, P., Jackman, A.L., 2006. Potentiation of paclitaxel activity by the HSP90 inhibitor 17-allylamino-17-demethoxygeldanamycin in human ovarian carcinoma cell lines with high levels of activated AKT. Mol. Cancer Ther. 5, 1197–1208.
Schwab, C.L., English, D.P., Black, J., Bellone, S., Lopez, S., Cocco, E., Bonazzoli, E., Bussi, B., Predolini, F., Ferrari, F., Ratner, E., Silasi, D.A., Azodi, M., Rutherford, T., Schwartz, P.E., Santin, A.D., 2015. Neratinib shows efficacy in the treatment of HER2 amplified carcinosarcoma in vitro and in vivo. Gynecol. Oncol. 139, 112–117.
Segovia-Mendoza, M., Gonzalez-Gonzalez, M.E., Barrera, D., Diaz, L., Garcia-Becerra, R., 2015. Efficacy and mechanism of action of the tyrosine kinase inhibitors gefitinib, lapatinib and neratinib in the treatment of HER2-positive breast cancer: preclinical and clinical evidence. Am. J. Cancer Res. 5, 2531–2561.
Staropoli, N., Ciliberto, D., Chiellino, S., Caglioti, F., Giudice, T.D., Gualtieri, S., Salvino, A., Strangio, A., Botta, C., Pignata, S., Tassone, P., Tagliaferri, P., 2016. Is ovarian cancer a targetable disease? A systematic review and meta-analysis and genomic data investigation. Oncotarget 7, 82741–82756.
Tian, K., Zhong, W., Zheng, X., Zhang, J., Liu, P., Zhang, W., Liu, H., 2015. Neuroleukin/Autocrine Motility Factor Receptor Pathway Promotes Proliferation of Articular Chondrocytes through Activation of AKT and Smad2/3. Sci. Rep. 5, 15101.
Wang, M., Zhang, Y., Wang, T., Zhang, J., Zhou, Z., Sun, Y., Wang, S., Shi, Y., Luan, X., Zhang, Y., Wang, Y., Wang, Y., Zou, Z., Kang, L., Liu, H., 2017. The USP7 inhibitor P5091 induces cell death in ovarian cancers with different P53 status. Cell. Physiol. Biochem. 43, 1755–1766.
Wilken, J.A., Webster, K.T., Maihle, N.J., 2010. Trastuzumab sensitizes ovarian Cancer cells to EGFR-targeted therapeutics. J. Ovarian Res. 3, 7.
Wissner, A., Mansour, T.S., 2008. The development of HKI-272 and related compounds for the treatment of cancer. Arch Pharm (Weinheim) 341, 465–477.
Wissner, A., Overbeek, E., Reich, M.F., Floyd, M.B., Johnson, B.D., Mamuya, N., Rosfjord, E.C., Discafani, C., Davis, R., Shi, X., Rabindran, S.K., Gruber, B.C., Ye, F., Hallett, W.A., Nilakantan, R., Shen, R., Wang, Y.F., Greenberger, L.M., Tsou, H.R., 2003. Synthesis and structure-activity relationships of 6,7-disubstituted 4-anilinoquinoline-3-carbonitriles. The design of an orally active, irreversible inhibitor of the tyrosine kinase activity of the epidermal growth factor receptor (EGFR) and the human epidermal growth factor receptor-2 (HER-2). J. Med. Chem. 46, 49–63.
Zhang, Y., Zhang, J., Liu, C., Du, S., Feng, L., Luan, X., Zhang, Y., Shi, Y., Wang, T., Wu, Y., Cheng, W., Meng, S., Li, M., Liu, H., 2016. Neratinib induces ErbB2 ubiquitylation and endocytic degradation via HSP90 dissociation in breast cancer cells. Cancer Lett. 382, 176–185.